Cost-benefit Tradeoff Mediates the Rule- to Memory-based Processing Transition during Practice

Guochun Yang[1,2,*] and Jiefeng Jiang[1,2,3,*]

[1] Cognitive Control Collaborative, University of Iowa, Iowa City, IA 52242, USA.
[2] Department of Psychological and Brain Sciences, University of Iowa, Iowa City, IA 52242, USA.
[3] Iowa Neuroscience Institute, University of Iowa, Iowa City, IA 52242, USA.
*Correspondence: guochun-yang@uiowa.edu (G.Y.) and jiefeng-jiang@uiowa.edu (J.J.)

Abstract

Practice not only improves task performance, but also changes task execution from rule- to memory-based processing by incorporating experiences from practice. However, *how* and *when* this change occurs is unclear. We tested the hypothesis that strategy transition in task learning results from cost-benefit analysis. Participants learned two task sequences and were then queried about the task type at a cued sequence and position. Behavioral improvement with practice can be accounted for by a computational model implementing cost-benefit analysis. Model-predicted strategy transition points are related to behavioral slowing and changes in fMRI activation patterns in the dorsolateral prefrontal cortex. Strategy transition is also related to increased pattern separation in the ventromedial prefrontal cortex. The cost-benefit analysis model outperforms alternative models (e.g., both strategies racing for being expressed in behavior) in accounting for empirical data. These findings support cost-benefit analysis as a mechanism of practice-induced strategy shift.

Keywords: cost-benefit tradeoff; practice; task representation; cognitive control; memory retrieval; pattern separation

Introduction

"Practice makes perfect". During task learning, practice improves performance and reduces effort. Practice effects occur in multiple cognitive functions supporting task execution. For example, it speeds up the processing of task-relevant information,[1,2]. Additionally, with practice task execution becomes more robust to distraction and requires less attentional control.[3,4] Crucially, practice also changes the strategy to perform a task. For example, Schuck et al.[5] observed that with practice participants spontaneously shift from a rule-based strategy to a less effortful strategy relying on task-irrelevant information. More generally, strategy switch can occur between two common types of strategies: those based on task rules and those based on experiences[6-9]. For instance, novice chess players must apply the rules to search for the best move, whereas experienced players can leverage their memory of previous games to recognize the board configuration to reduce the effort of searching and retrieving the best move.[10-12] This transition from rule-based processing to memory-based retrieval is termed automatization and is vital in learning complex tasks (e.g., chess, programming and arithmetic).[13,14] However, little is known about *when* and *how* this transition happens.

Motivated by theories of the cost-benefit analysis in the control of goal-directed behavior,[15,16] our guiding hypothesis is that the transitions in strategy during task performance likely reflect the optimization of cost-benefit tradeoff. Conceptually, a memory-based strategy retrieves the answer directly and bypasses the execution of the rules. Thus, it is less effortful/costly than a rule-based strategy. However, the memory-based strategy depends on the accumulation of experience, meaning its benefit starts off low and gradually increases as the memory becomes stronger with practice. In contrast, the benefit of rule-based processing remains consistently high from the outset. Therefore, early in task learning (e.g., a novice chess player), the rule-based strategy is favored because its higher benefit outweighs its higher cost compared to the memory-based strategy. As more experience is gained (e.g., a veteran chess player), the increased benefit makes the memory-based strategy outperform the rule-based strategy in the cost-benefit tradeoff, leading to a strategy transition from rule- to memory-based processing. The memory-based strategy remains the winning strategy afterwards. We call this the cost-benefit tradeoff model. Alternatively, different strategies could be implemented simultaneously in a competitive manner akin to a horse race, where the strategy that first reaches a predefined threshold dictates performance.[13,17] We refer to this as the horse-race model. Additionally, humans may intrinsically prefer a one-step retrieval strategy, applying it whenever the memory is strong enough to retrieve instances from memory.[18] We term this approach the memory-threshold model. How each model explains the change of the winning strategy as memory strengthens with practice is illustrated in Fig. 1A.

To adjudicate between these competing models, we designed a two-phase experiment. Human participants (n = 33) learned two different task sequences involving the same component tasks in the training phase (Fig. 1A; each task sequence consists of five distinct delayed matching tasks, see Materials and Methods).

In the following test phase, participants were asked to report the task type at a cued position from one sequence (e.g., A4, denoting the 4th position in sequence A) while undergoing fMRI scanning (Fig. 1B). As detailed above, the cost-benefit analysis model predicts that participants would start with a rule-based strategy (i.e., by recalling the task sequence learned from the training phase to identify the cued task) and switch to the memory-based strategy when the retrieval of cue-task associations becomes more efficient than sequence recall with practice (Fig. 1C).

To preview the results, we constructed several computational models and found that the cost-benefit tradeoff model outperforms the memory-threshold model in accounting for behavioral data. To compare the cost-benefit analysis model to the horse-race model, we focused on their key difference: the former posits that only the strategy with the best cost-benefit tradeoff is implemented, whereas the latter assumes both strategies are simultaneously implemented and hence there is no strategy switch. Three findings support the cost-benefit analysis model over the horse-race model: (1) slowed responses following model-predicted strategy transition points, (2) selective fMRI representation of the winning strategy rather than both strategies, and (3) fMRI representation of the decision variable of the cost-benefit analysis.

To gain insights into the neural substrates of the cost-benefit analysis model, we focused on fMRI signal change around strategy transitions and found that the right dorsolateral prefrontal cortex (dlPFC) encodes the current winning strategy. Linking the improved memory to strategy transition, we observed that the ventromedial PFC (vmPFC) tracks the increase of the memory strength of cue-task associations. In summary, these findings reveal that strategy selection is driven by a dynamic cost-benefit analysis, and the strategy transition occurs when the value (i.e., cost-benefit tradeoff) of the memory-based strategy outweighs that of the rule-based strategy.

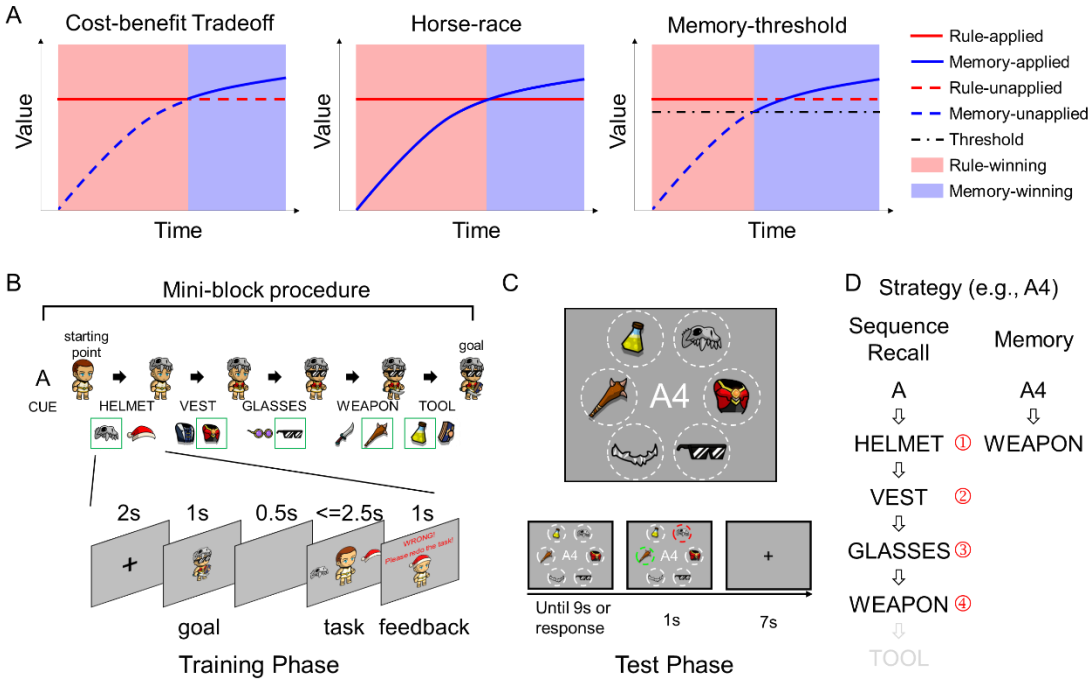

Figure. 1. Competing models and the experimental design. A) Three competing models and how improved memory due to practice affects strategy application. In the

cost-benefit analysis model, the memory-based strategy replaces the rule-based strategy when the former has better values (i.e., cost-benefit tradeoff). In the horse-race model, both strategies are always implemented. In the memory-threshold model, the strategy switches to memory-based when the memory strength reaches a pre-defined threshold. B) Design of the training phase. Top panel: During the training phase, participants learned two sequences of tasks (one example sequence shown) with practice. Each sequence consists of five different tasks in a fixed order, indicated by a cue (A or B) presented before the first trial of the corresponding sequence. Each task requires the participant to equip an avatar with a specific type of gear (e.g., helmet). Bottom panel: A task starts with a goal image and then two option gears, one on each side of an avatar. Participants are required to choose the gear that matches the goal image. The goal image was randomized for each mini-block to ensure that the sequences are defined by equipment types (e.g., weapon) rather than specific stimuli (e.g., dagger). C) Design of the test phase. Top panel: During the test phase, a cue denoting the position from a sequence (e.g., A4, denoting the 4th position in sequence A) is displayed in the center of the screen. Surrounding the cue are six equipment pictures denoting five task types plus a foil (MOUSTACHE), with their spatial locations fixed but their equipment options randomly selected. Participants are required to identify the task type at the cued position of the sequence by selecting the equipment representing the task type (e.g., nunchaku, representing the weapon task). Bottom panel: trial time course. D) Illustration of the two strategies. The rule-based strategy would recall the cued sequence (e.g., A) from the first position till the cued position (e.g., 4), whereas the memory strategy would retrieve the association between the cue (e.g., A4) and the task (e.g., weapon) directly.

Results

The results are organized into two parts: The first part compares the cost-benefit analysis model to alternative models (Fig. 2-3, Table 1). The second part investigates the neural substrates and their behavioral significance of the key components of the cost-benefit analysis model (Fig. 4-7).

Model-free behavioral results

In the training phase, participants were trained until they accurately (with accuracy > 90%) remembered transitions between tasks (see Methods). For test phase data, we first conducted a model-free analysis. Trial-wise response times (RTs) and error rates (ERs) were analyzed separately using linear mixed effect (LME) models. Predictors included cued position (1–4), block (1–6) and their interaction. RT results (Fig. 2A) showed a significant main effect of block (β = –0.33, SE = 0.03, 95% confidence interval (CI) = [–0.39 –0.28], $t(33.3) = -11.41$, $p < .001$, $\eta_p^2 = .40$), a significant main effect of position (β = 0.48, SE = 0.05, 95% CI = [0.38 0.59], $t(33.0) = 9.68$, $p < .001$, $\eta_p^2 = .58$), and a significant interaction effect (β = –0.10, SE = 0.02, 95% CI = [–0.14 –0.07], $t(59.8) = -5.73$, $p < .001$, $\eta_p^2 = .06$). Post-hoc comparisons showed that the linear effect of position in block 1/2 was larger than block 2−6/4−6, respectively (*p*s <

.05). ER results showed a significant main effect of block (β = –0.20, SE = 0.05, 95% CI = [–0.29 –0.10], t(33.0) = –4.17, p < .001, η_p^2 = .06), position (β = 0.20, SE = 0.05, 95% CI = [0.11 0.30], t(36.6) = 4.41, p < .001, η_p^2 = .06), and a significant interaction effect (β = –0.13, SE = 0.04, 95% CI = [–0.21 –0.04], t(40.4) = –3.09, p = .004, η_p^2 = .02). Post-hoc comparisons suggested that the linear effect of position in block 1 was larger than block 3 and 6, in block 2 than in block 3,4 and 6, and in block 5 than in block 6, ps < .05. We also replicated these findings using all five cued positions (Supplementary Note S1). Overall, we observed three patterns: (1) performance, when collapsed across cued positions, improved over time; (2) performance, when collapsed across blocks, was worse when the later sequence positions were cued; and (3) this negative association between performance and cued position decreased with time.

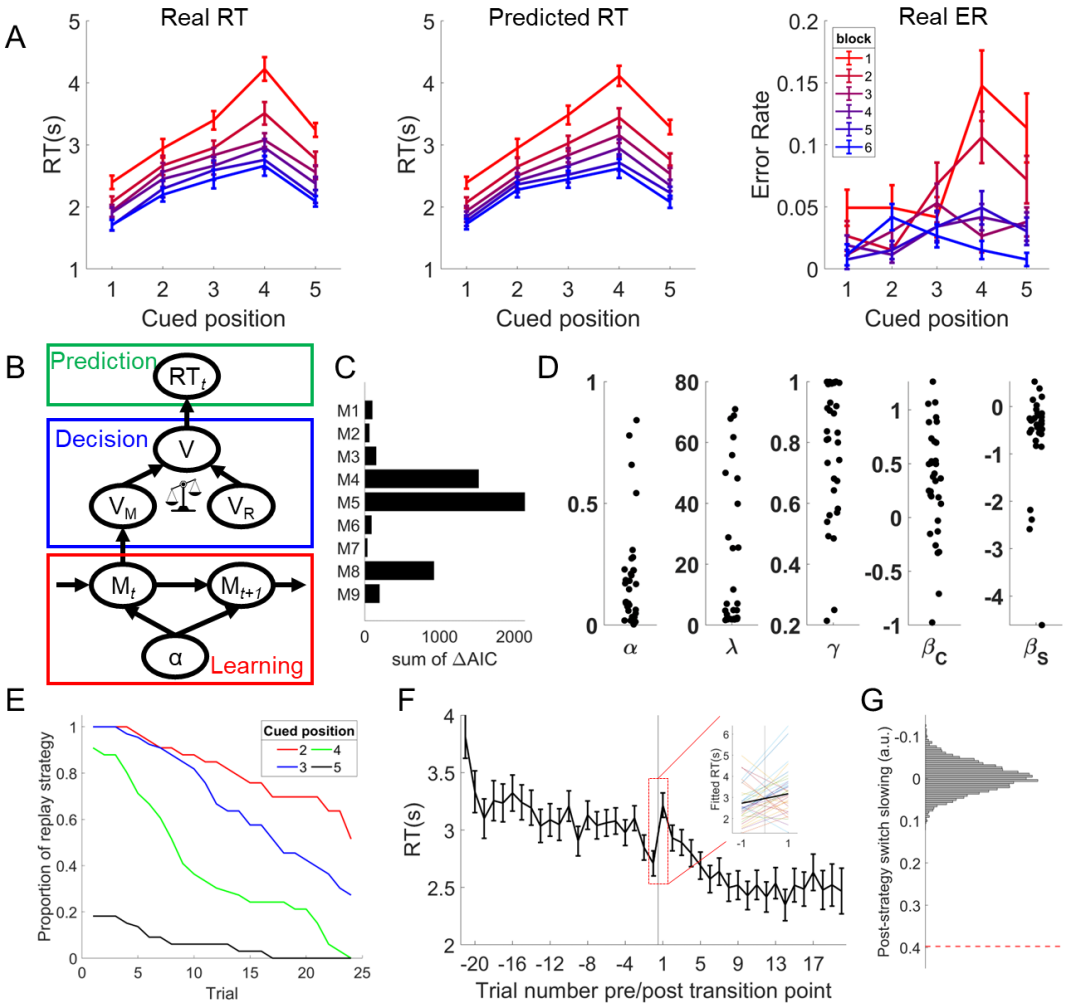

Figure 2. Behavioral and computational modeling results. A) behavioral data (RT, left panel, and ER, right panel) and model predicted RT (middle panel) displayed as a function of cued position and block. Error bars denote standard errors of the mean (SEMs). B) The structure of the generative model. It includes three main components: learning, decision, and prediction. The learning component updates the memory strength of the cue-task associations (i.e., a probabilistic distribution of the correct task, denoted as M) using a delta rule with learning rate α. The decision component makes winner-take-all decisions about which strategy to apply using cost-benefit

analyses. The prediction component predicts trial-wise RT based on linear predictors of values driven by rule- (V_R) or memory-based (V_M) strategies, depending on the strategy used. The model was fit to trial-wise RT data to estimate model parameters and trial-wise prediction of the strategy used. C) Model comparison based on the group-level ΔAIC (Akaike information criteria), i.e., increased AIC of alternative models (see Table 1 and Methods) compared to the winning model (Model0, illustrated in panel B). D) Individual model-estimated parameters (α = learning rate, λ = cost-benefit tradeoff, γ = recency effect, see definition in Materials and Methods) and beta coefficients for rule implementation cost (C) and memory strength (S) effects. E) Change of model predicted strategy over time. The Y axis shows the model-inferred proportion of participants using the rule-based strategy. Trials were counted for each cue separately. F) The RT as a function of trial number relative to the cue's transition point. The inset highlights the increase of RT on the trial following the estimated strategy switch. Error bars denote SEMs. G) Post-strategy switch slowing of real data (dashed red line) and its null distribution (histogram) estimated using randomly selected transition points.

Model-based behavioral results

We constructed several computational models to capture the dynamics of transitioning from rule- to memory-based strategy (Fig. 2B and Materials and Methods). Our first model is a quantitative version of the cost-benefit tradeoff model. On each trial, the model performs a cost-benefit analysis to determine which strategy to use based on their values, defined as a weighted sum of cost and benefit. Conceptually, the rule-based strategy retrieves a task before the cued position (e.g., the first task of a sequence) and recalls later tasks using sequential memory until the cued position is reached. On the other hand, the memory-based strategy directly retrieves the cued task through cue-task associations. Thus, the rule-based strategy is more effortful (and thus costly) than the memory strategy. Early in the test phase, the cue-task association was weak, whereas the participants had strong sequential memory of the task order from the training phase. Thus, the rule-based strategy provides better value than the memory strategy due to its higher benefit (despite of higher cost) and is favored. As participants received feedback with practice, the cue-task association became stronger. Along with its smaller effort compared to replay, the memory-based strategy eventually achieved a higher value, leading to the transition of strategy.

Based on the trial-wise model prediction of which strategy to use, trials were categorized as rule and memory trials. For each participant, the model outputs were then linked to trial-wise RT using a linear model (M0, Table 1) with the following regressors: (1) rule implementation cost (C, number of steps from recalling start to cued position) for rule trials, (2) the strength of the cue-task association (S) for memory trials, quantified as the reversed entropy of the task distribution conditioned on the cued position, (3) trial type (i.e., rule ($Type_R$) vs. memory ($Type_M$)), (4) the interaction between C and aggregated times of rule implementation since the beginning of the experiment ($C*Times_R$) that reflects the practice effect of replay (i.e., more experience would accelerate sequence recall and reduce the effect of C on RT),

(5) log-transformed trial number that reflects practice effect not involving strategy switch and (6) response (dummy coded). We compared M0 to its reduced versions (Table 1, M1-M5) using likelihood ratio tests at the group level. M0 outperformed all other models (*p*s < 0.001, Fig. 2C). Of note, the two reduced models that assume either rule-based strategy only (M4, with only C) or the use of neither rule- or memory-based strategy (M5, without C or S) were outperformed by all other models that assume two strategies (*p*s < .001), suggesting that both strategies were used. These results suggest that all components in M0 are important to account for behavior.

We then compared M0 to other alternative models. First, to test whether the behavioral performance considers the improved efficiency in the cost-benefit analysis, as indicated by the interaction effect of C*Times$_R$, we compared M0 to a new model (M6, Table 1 and Supplementary Note S2). Comparison between unnested models was achieved through Akaike information criteria (AIC). The results showed that M6 (AIC = –3928) performed worse than M0 (AIC = –4019), $p < .001$, suggesting no evidence of such consideration. Second, we also explored the possibility of applying a backward sequence recall strategy with model M7, where recall could start from the last position and progress backward to the cued position (akin to backward replay). This model (AIC = –3984, worse than that of M0, $p < .001$) was not supported by behavioral data (Table 1 and Supplementary Note S3). Third, we tested whether the cost-benefit analysis was probabilistic (i.e., strategy can switch back and forth) using a variant of M0 (M8, see *Methods and Materials*). M8 performed worse (AIC = –3095) than M0 (Table 1, $p < .001$). Finally, to compare M0 to the memory-threshold model, we developed another model (M9) without the cost-benefit analysis. This model predicts strategy switches when the memory strength reaches a threshold. However, M9 performed worse (AIC = –3823) than the M0, $p < .001$ (Table 1). As the model is trained by observed behavior, it cannot distinguish between whether the behavior results from the implementation of a selected strategy or a competition among different implemented strategies. Consequently, the horse-race model exhibits the same structure as the cost-benefit tradeoff model. To dissociate the two models, we compared them using behavioral and fMRI data (see below).

As M0 was the winning model, it was used for all subsequent future analyses. Individual model parameters from M0 are shown in Fig. 2D. The effect of C was significantly above 0 ($\beta = 0.33$, SE = 0.09, Cohen's d = 0.64, 95% CI = [0.15 0.51], $t(32) = 3.70$, $p < .001$), indicating that participants were slower when the model predicted more steps to recall. The interaction between the simulation cost and the accumulated rule-based trials was significant ($\beta = -0.09$, SE = 0.04, Cohen's d = –0.38, 95% CI = [–0.18 –0.01], $t(32) = -2.20$, $p = .035$), suggesting that sequence recall accelerated over time. The memory strength effect (S) was also significant ($\beta = -0.61$, SE = 0.17, Cohen's d = –0.61, 95% CI = [–0.96 –0.26], $t(32) = -3.52$, $p = .001$), suggesting that participants responded faster when the model predicts a stronger cue-task association on memory trials. Based on this model, the predicted proportion of participants using the rule-based strategy decreased over time (Fig. 2E), indicating that the rule-based strategy was replaced by the memory strategy with

practice. We defined transition points as immediately before the trial on which the value of the memory strategy first surpassed the rule-based strategy (Fig. S2A). Transition points were defined for each cue except for cues at position 1 because for that position no transition was necessary. Among the remaining 192 trials for cued positions 2–5, the model predicted that a participant applied the rule-based strategy on 94 ± 37 trials, varying from 21 to 166 trials.

Table 1. Description of tested models and corresponding model comparison results.

Model regressors	M0*	M1	M2	M3	M4	M5	M6	M7	M8	M9
C_forward	+	+	+	+	+	–	–	+	+	+
C_forward discounting	–	–	–	–	–	–	+	–	–	–
C_backward	–	–	–	–	–	–	–	+	–	–
S	+	+	+	+	–	–	+	+	+	+
Type (R/M)	+	–	+	–	–	–	+	+	+	+
C_R*$Times_R$	+	+	–	–	+	–	+	+	+	+
Comparison between strategies	+	+	+	+	–	–	+	+	+	–
Probabilistic / **D**eterministic	D	D	D	D	D	D	D	D	P	D
AIC	–4019	–3917	–3959	–3866	–2497	–1878	–3928	–3984	–3095	–3823
Compared with M0 (p value)		< .001	< .001	< .001	< .001	< .001	< .001	< .001	< .001	< .001

Note. The predictors of logged trial number and response were included in all models and are hence not reported in model comparison. C = cost of rule implementation; S = memory strength; R = rule trial; M = memory trial; AIC = Akaike information criteria. Specifically, M0 represents settings of the cost-benefit tradeoff model, and M9 represents the memory-threshold model. * denotes the winning model.

Behavioral slowing following model-predicted strategy transition

To validate the transition points predicted by the model, we tested the strategy switch cost following the transition point.[19] Using an LME model, we observed a significant increase of RT after transition points (β = 0.40, SE = 0.15, 95% CI = [0.10 0.69], $t(80.5) = 2.64$, $p = .0010$, $\eta_p^2 = .15$, Fig. 2F). To examine further whether this effect is reliably linked to the model-predicted transition points, we repeated this analysis 5,000 times using randomly selected transition points for each cue and each subject. The observed post-switch slowing was greater than all random ones ($p <$ .001, Fig. 2G). It is noteworthy that this effect is independent of the model fitting, which only assumes that the mean RT for memory and rule trials can be different (i.e., different intercepts), without any assumptions involving the two adjacent trials of the

transition point. We further tested the alternative explanation that the structure of the computational model is biased to reporting artificial post-transition slowing. To this end, we repeated the post-transition slowing analysis using randomly sampled model parameters while keeping the architecture of the model constant 5,000 times. The median of the resulting distribution was centered around 0 and significantly lower than the observed post-switch slowing, $p = .005$ (Fig. S2B), thus ruling out the possibility that the model artificially introduced a post-switch slowing effect.

Importantly, the horse-race model assumes no strategy transition, as both strategies are always executed. It follows that RT was not expected to change systematically following the transition point identified by the cost-benefit tradeoff model. Thus, the post-switch slowing phenomenon provides evidence supporting the cost-benefit tradeoff model over the horse-race model.

Selective activation of winning strategies in fMRI data

We next compared the cost-benefit tradeoff model and the horse-race model using fMRI data. The former assumes that only the winning strategy is implemented on each trial. On the other hand, the latter assumes that both strategies are always implemented. Therefore, we next tested whether fMRI activation patterns selectively encode the rule- and memory-based strategy for rule and memory trials, respectively. For the rule-based strategy, we predicted that the similarity of fMRI activation patterns across two trials would reflect the number of shared recalled tasks (Fig. 3AB). For the memory-based strategy, we tested the cue effect such that the two trials' activation patterns will be more similar if they share the same cue than not, as the cue and its association with the task are used in the memory strategy (Fig. 3AC). The cost-benefit tradeoff model predicts a stronger rule effect on rule than memory trials and a stronger cue effect on memory than rule trials, whereas the horse-race model predicts both strategies are activated regardless of the trial type.

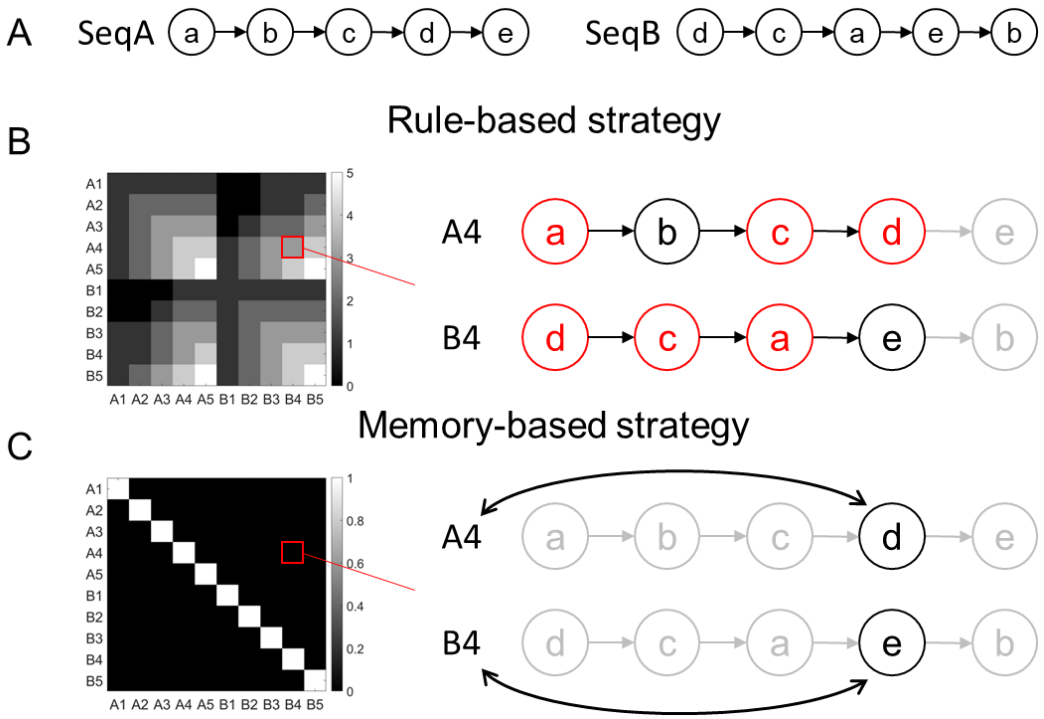

Figure 3. Coding schemes of representational similarity for rule- and memory-based effects. A) The two task sequences. Letters a-e represent the five tasks. B) The hypothetical representational similarity for rule effect is quantified as the number of shared recalled tasks between two trials. For example, cues A4 and B4 share three tasks in rule implementation, namely a, c and d (red nodes), resulting in a similarity level of 3. C) The hypothetical representational similarity for the cue effect (reflecting memory strategy) is defined by the concordance of the cues and hence their associated tasks. For example, the cues A4 and B4 are different, thereby yielding a similarity value of 0. The light gray nodes and arrows in panels B and C indicate the tasks that are neither sequentially recalled nor retrieved by cue.

Results showed widespread brain regions with a stronger rule effect on rule trials than memory trials (Fig. 4A-B) and the opposite pattern for the cue effect (Fig. 4D-E). To statistically test the strength of each effect across trial types while controlling for processing shared by both strategies (e.g., visual processing), we compared each effect between rule and memory trials. A stronger rule effect on rule trials compared to memory trials was observed in the striatum, frontoparietal, temporal and occipital regions (Fig. 4C, *p*s < 0.05 corrected), whereas a stronger cue effect on memory than rule trials was found in similar regions with less spatial extent (Fig. 4F, *p*s < 0.05 corrected). No regions showed a statistically significant effect in the opposite direction in either test. A conjunction analysis identified a double dissociation between trial type and strategy in frontoparietal, temporal, occipital and subcortical regions (Fig. 4G, see Table S1 for a detailed list of brain regions and statistics). We replicated these findings after regressing out the difficulty of different conditions with a covariate of the RT difference in the regression model (see Fig. S6). The double dissociation supported the cost-benefit tradeoff model by showing selective activation

of the winning strategy from the cost-benefit analysis. On the other hand, the horse-race model was not supported, as we did not observe any brain region showing both rule and cue effects on both rule and memory trials. In particular, no brain regions showed a rule effect on memory trials (Fig. 4B).

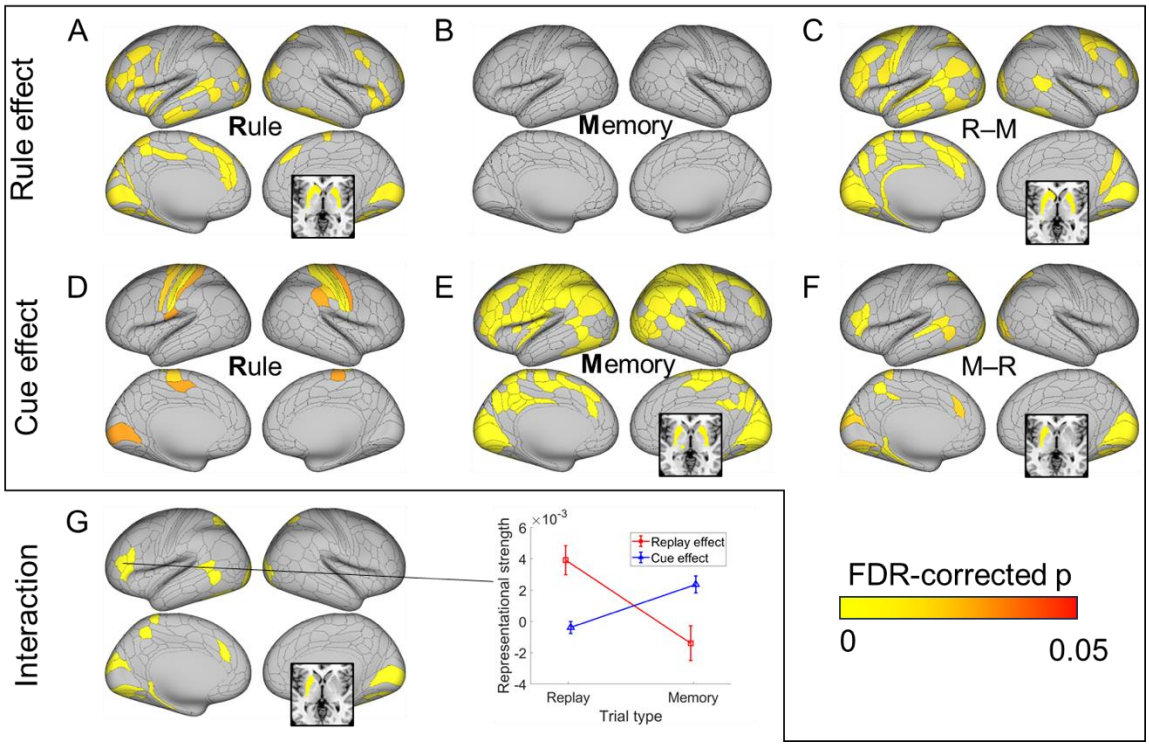

Figure 4. Double dissociation of rule and memory representations on their respective trials revealed by multivariate activation patterns. A significant representation of rule effect is observed on rule (R) trials (panel A) but not on memory (M) trials (panel B). C) A stronger rule effect on rule than memory trials (R–M) was found in frontoparietal, temporal, occipital and subcortical regions. In contrast, the cue effect was exhibited in more regions on memory trials (panel E) than in rule trials (panel D), and regions showing a stronger memory effect on memory than rule trials (M–R) include frontoparietal, temporal, occipital and subcortical regions (panel F). G) Regions showing double dissociation (i.e., the conjunction of C and F) with both stronger rule effect representation in rule trials and stronger cue effect representation in memory trials. The middle panel illustrates the double dissociation with an example region (left inferior prefrontal sulcus, IFSa). All subcortical regions are depicted in an axial slice at z = 0.

Neural coding for key variables of the cost-benefit analysis model

After showing that the cost-benefit analysis model better accounts for behavioral and fMRI data than alternative models, we conducted a multivariate analysis of fMRI data to test the encoding of its key variables.[20] A similar analysis using univariate fMRI methods is reported in Supplementary Note S6 and Fig. S3. For the rule-based strategy, we tested the variable of cued position, as later cued position is related to higher rule implementation cost (e.g., more tasks to sequentially recall, higher

difficulty and higher working memory load). We found that this variable was encoded in the left IFSa, $p < .05$, FDR corrected (Fig. 5AD). On the other hand, for the memory-based strategy, we tested the encoding of the memory strength of cue-task associations (Eq. 3) and found that memory strength was encoded in primary visual regions (bilateral V1, V2, right V3, right V4), sensorimotor regions (left primary motor area, left lateral 8B, right area 2), temporoparietal junction regions (left PF complex, left intraparietal 2, right PFm complex, right medial intraparietal area), among others (left rostral area 6, left auditory 5 complex, right middle TE1 and right dorsal 32), all *p*s < .05, FDR corrected (Fig. 5BD). In addition, given the importance of the posterior parietal cortex in memory retrieval,[21] we also tested the memory strength effect in bilateral PFm, PGs, and PGi, and results showed four of the six regions (bilateral PGs, right PFm and right PGs) reached significance, *p*s < 0.03, Bonferroni corrected.

To test the presence of the cost-benefit analysis process predicted by the cost-benefit tradeoff model, we searched for brain regions encoding the decision variable, defined as the absolute value difference between the two strategies. We expected to observe this effect in the dorsomedial prefrontal area.[15] Consistently, the right 8BM and right supplementary and cingulate eye field (SCEF) showed significant decision variable effect, *ps* < .05, FDR corrected. In addition, this effect was also observed in primary visual regions (bilateral V1-V4), sensorimotor regions (bilateral areas 1, 2, 3b, 4, right 3a, bilateral dorsal area 6, bilateral 24dd, right 7AL), as well as other areas such as the right anterior area 6, right anterior part of inferior frontal junction (IFJa), right PF complex and right A4, *p*s < .05, FDR corrected (Fig. 5CD).

Brain-behavioral correlation of memory-based strategy

We next examined the explanatory power of the cost-benefit tradeoff model by investigating whether the model-fitting results could be linked to the neural findings. The model fitting yielded a λ parameter that reflects the preference for a memory-based strategy. A smaller λ value corresponds to a relatively higher value of the memory-based strategy (see Methods). Therefore, we predicted that a smaller λ would be correlated with stronger encoding of memory strength in the brain. To test this prediction, we calculated the average memory encoding strength across regions showing statistically significant representation of memory strength (Fig. 5B). Our analysis revealed a negative correlation between λ (log-transformed) and encoding strength, $r = -0.52$, $p = 0.001$, one-tailed, uncorrected (Fig. 3E). This negative correlation was observable in 3 out of 17 regions (bilateral V1 and left PF), *p*s < 0.05, one-tailed, FDR corrected, with the strongest correlation in the left PF, $r = -0.50$, $p = 0.026$, one-tailed, FDR corrected (Fig. 5F). Thess results suggest that the extent to which individuals prioritize the memory strategy is related to their neural sensitivity of memory encoding.

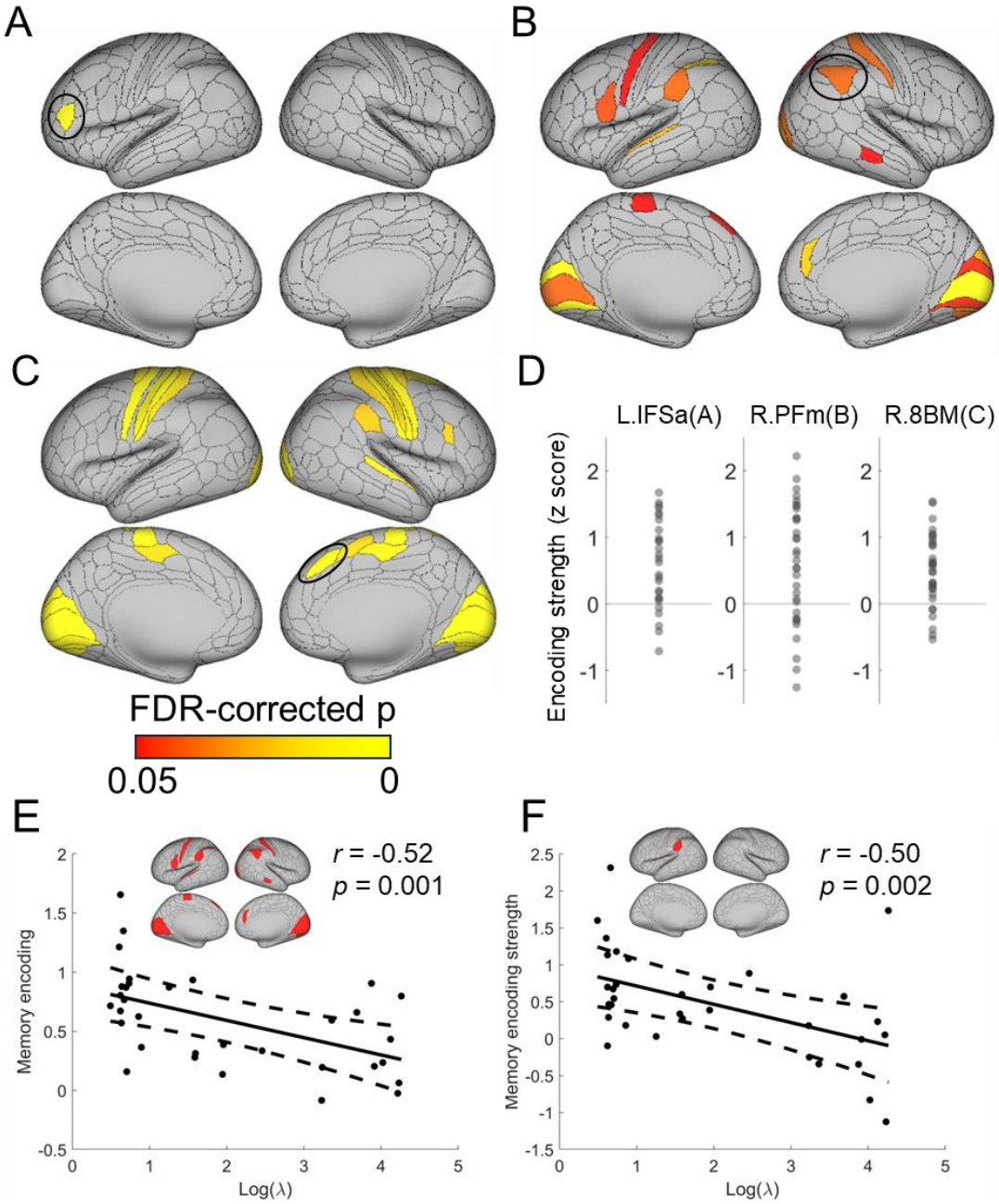

Figure 5. Multivariate encoding of rule-, memory-based strategies and the decision variable. A) The left inferior prefrontal region encodes the cued position, reflecting the cost of rule implementation. B) The memory strength is encoded in the visual area, sensorimotor and temporoparietal association regions. C) The decision variable is encoded in sensorimotor and dorsomedial prefrontal regions. D) The encoding strength of three representative regions (highlighted by black ovals in A-C) for the cued position (left), memory strength (middle) and decision variable (right). Each dot indicates one subject. E) and F) show a negative correlation between the model prediction of the cost-benefit tradeoff factor (log-transformed λ) and the neural memory encoding strength from those brain regions identified in B) on average, and a single region left PF for example, respectively.

Dorsolateral PFC encodes boundary effect across the transition point

Our behavioral and modeling results suggest an abrupt shift of strategy when the value of memory retrieval outweighs the rule implementation (Fig. 2F and Fig. S2A). We anticipated that there are neural substrates sensitive to this abrupt shift,[5,22] distinct from the overall differences observed during the constant application of the two strategies (Fig. 5). Therefore, we next aimed to identify the brain regions supporting the strategy switch. To this end, we treated a transition point as a boundary separating the two time periods using different strategies. We then tested the boundary effect (i.e., higher pattern similarity between trials at the same side of the boundary than different, termed as "within boundary" and "between boundary" conditions, respectively). To focus on the effects specific to the boundary, we compared pattern similarity of the trials immediately adjacent to the transition point and other temporally close trials (i.e., between 2 and 6 trials away from the transition point). We excluded trial pairs involving different cues to prevent potential confounding effects from intrinsic differences across cues (Fig. 4C). We found that the right Dorsolateral PFC (dlPFC region, area p9-46v) showed a statistically significant boundary effect (Fig. 6, β = 0.0109, SE = 0.0028, 95% CI = [0.0054 0.0165], t(1358.0) = 3.86, p = .023 corrected, η_p^2 = .0116). No other regions survived the correction for multiple comparisons. This effect was stronger than its null distribution using shuffled transition points 5,000 times (p = .024, Fig. 6C), suggesting that the boundary effect is tied to the model-estimated transition points. To further rule out the possibility that this finding captured a generic trial-type effect (i.e., independent of the trials' temporal distance from the transition points), we repeated the same analysis by replacing the temporally close trials with trials that were more than 6 trials away from the transition point and did not observe the boundary effect (t(30.7) = 0.84, p = .203 uncorrected). In other words, it appears that this effect only occurred on trials near strategy transition and supports the relation between dlPFC representation and strategy transition.

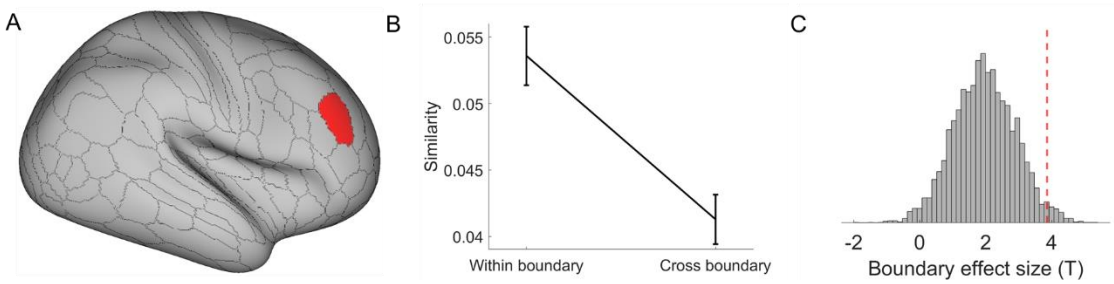

Figure 6. Dorsolateral PFC encodes the boundary effect across the transition point. A) The right p9-46v shows a higher within-boundary than cross-boundary pattern similarity for trials around the transition points. B) Pattern similarity (group mean ± SEM) as a function of within/cross-boundary in the region right p9-46v. C) The significant boundary effect (i.e., the higher pattern similarity within-boundary

than cross-boundary condition, indicated by the red dashed line), compared with a null distribution obtained by randomly shuffling the transition point 5,000 times.

Ventromedial PFC pattern-separates cue-task associations

As the cost-benefit analysis model considers the improvement in memory strength as the driving factor of the strategy switch, we tested the increase in memory strength using pattern-separation[23] as an operationalization. In other words, we predicted that pattern similarity between different cues is expected to reduce over time. To focus on strategy transition, trials were time-locked to their corresponding transition points. Trial positions containing too few (< 30) data points were excluded from the analysis. The predicted decrease of between-cue pattern similarity was observed in the left ventromedial PFC (vmPFC, 10r area, Fig. 7AB, $t(52.4) = -3.93$, $p < .001$, $p = .048$ corrected, $\eta_p^2 = .2279$). No other regions survived the correction for multiple comparisons. Moreover, to explore the possibility that vmPFC displays a generic decrease of between-cue pattern similarity over time, we repeated this analysis 5,000 times with randomly selected transition points. These randomized data maintain the chronological order of trials. This, the generic decrease hypothesis would predict the effects in the repeated analysis to be similar to the observed effect. Results showed that the pattern separation observed in the left vmPFC (i.e., the negative slope β) falls below all values in this distribution, $p < 0.001$ (Fig. 7C). This rules out a possibility of bias due to a time effect. Together, the results suggest that the vmPFC separates neural representations of different cue-task associations during task learning, potentially strengthening these associative memories via reducing interference between associations.

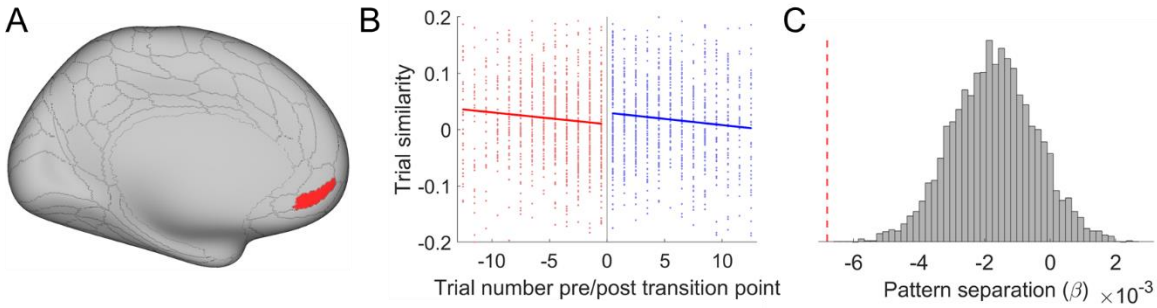

Figure 7. Ventromedial PFC pattern-separates cue-task associations. The left 10r area shows that pattern similarity among different cues decreases over time. A) The anatomical location. B) A scatter plot of trial similarity as a function of trial number relative to the transition point and the corresponding fitting lines. Red and blue colors indicate rule and memory trials, respectively. C) The significant pattern separation effect (i.e., the negative coefficient, indicated by the red dashed line) compared with a null distribution obtained by randomly shuffling the transition point 5,000 times.

Discussion

Practice improves task performance not only by making task execution more efficient but also by changing the strategy in which the task is performed. Here, we investigated how task strategy and related neural representations change in task learning. After learning two task sequences, participants were asked to report the task type at a cued position from one sequence. The behavioral data show worse performance for later cued positions, suggesting that participants adopted a strategy to recall (via forward replay) the task sequence to obtain an answer. Additionally, the strength of the performance-cued position correlation decreases over time, which can be explained by a transition to a memory-based strategy that retrieves the cued task directed from memory (i.e., performance is not sensitive to cued position). We tested *how* and *when* the transition occurs with computational modeling, and found evidence for the model that chooses the strategy via cost-benefit analysis. This model outperformed a memory-threshold model, which predicts strategy transition occurs whenever the memory strength of cue-task associations surpasses a certain threshold. We also considered a horse-race model, which posits that (1) both strategies are always implemented to compete for driving the response and (2) there is no strategy transition. On the other hand, the cost-benefit tradeoff model assumes (1) only the winning strategy is implemented and (2) that strategy switches will occur based on the cost-benefit analysis. In comparing the predictions, we found that fMRI data revealed a selective representation of the winning strategy (Fig. 4) and the representation of the decision variable (Fig. 5C), and behavioral data exhibited a post-transition slowing effect (Fig. 2F). Both sets of findings clearly support the cost-benefit tradeoff model. We then delved into the cost-benefit tradeoff model and found that strategy transition is related to the shift in neural representation in the dlPFC (Fig. 6) and associated with a gradual pattern separation in the vmPFC (Fig. 7).

These findings highlight *when* the transition between rule- and memory-based strategies would occur. Our computational model reconciles the gradual increase in pattern separation in neural data (Fig. 7, also see ref[24]) and the abrupt strategy switch (Fig. 2F, also see ref[5]) by introducing trial-level cost-benefit analysis between the two strategies. In other words, as the cue-task associations strengthen, the cost-benefit tradeoff (i.e., value) for the memory strategy increases gradually and monotonically (Fig. S2A). When it starts to achieve a better cost-benefit tradeoff than rule implementation, subsequent trials will use the memory strategy. The estimated transition points were validated by independent analyses of post-transition slowing (Fig. 2F and S2B) and the boundary effect in the dlPFC (Fig. 6). These model-based findings not only document a strategy shift in practice-induced automaticity,[13] but also provide a new account to *how* it occurs. Specifically, model comparison results (Table 1) highlight the importance of cost-benefit tradeoffs in the human brain's decision-making process when choosing between alternative strategies.[15,25,26] We further observed that the decision variable of the cost-benefit analysis may be encoded in the dmPFC (Fig. 3C). This is consistent with the finding that dmPFC accumulates

information prior to strategy shift,[5] such that in our work the cost-benefit analysis provides the information to switch strategy.

A group of brain areas seems to represent both strategies (Fig. 4). This may seem contradictory to the assumption that there were two distinct strategies. We argue that although the two strategies lead to the response in different ways, they indeed share some common cognitive processes, such as visual processing of the cue, memory retrieval and response production. Thus, the same brain regions can be involved in some processes that support both strategies. Crucially, we showed a double dissociation in a subset of these regions, such as the frontoparietal regions (Fig. 4G), such that their activation patterns changed with the strategy. This suggests that these brain regions support the two strategies in different ways. Of note, the recalling of a task from learned sequences suggests that sequential replay is part of the rule-based strategy.[27,28] To test this, we conducted a multivariate classification analysis to decode tasks that can be replayed (i.e., tasks prior to the cued task). We found that these tasks could indeed be decoded from regions such as left dlPFC only in rule trials but not in memory trials, and that in frontoparietal and visual areas these tasks could be better decoded in rule than memory trials (Supplementary Note S8, Fig. S7), thus supporting the assumption of forward replay through the task sequences.

When focusing on behavioral and neural changes related to strategy transition, we first observed a behavioral post-transition slowing effect (Fig. 2F) and a numerical trend of increased fMRI activation in the prefrontal cortex following estimated transition points (Fig. S4). We further found that dlPFC activation patterns are different before and after strategy transition (Fig. 6). This difference is specific to trials near the transition point instead of reflecting the difference between the two strategies per se. This boundary effect may signal the establishment of an event boundary[22,29] that segments experiences based on the strategy used to reduce the interference from the rule-based strategy after the strategy transition.[30] In other words, we speculate that the right dlPFC may encode two contexts to host cognitive control information to guide the execution of different strategies. This is in line with our prior work documenting the right dlPFC encoding context-specific cognitive control information in a task switching paradigm[30] and organizing different types of cognitive control information.[31]

Pattern separation is a fundamental mechanism for organizing the memories of multiple similar items.[23] We showed that with practice, the neural pattern similarity across different cues was gradually reduced (Fig. 7), implying an increasingly pronounced pattern separation. This finding is in line with recent research illustrating robust pattern separation over time during the learning process.[24] We identified the most robust pattern separation in the left ventromedial frontal region,[32] underscoring the significance of the vmPFC in episodic memory,[33] pattern separation,[34] prospective memory[35] and concept construction.[36]

In conclusion, the present study demonstrates *how* and *when* a transition from a rule-based to a memory-based strategy occurs during practice to improve performance and reduce effort. The strategy transition occurs when the value of a memory-based strategy outweighs the rule-based strategy based on a cost-benefit analysis. This

process is characterized by a selective representation of a more efficient strategy at any given time, which, while optimizing performance, introduces an event boundary and a cost of transition between different strategy phases. These findings extend our understanding of how practice is associated with neural and behavioral changes in how tasks are represented and executed to improve performance.

Acknowledgement

This project was supported by the National Institute of Mental Health (R01MH131559 to J.J.). This work was conducted on an MRI instrument funded by S10RR028821. We thank Tobias Egner, Tammy Tran, Kai Hwang, Jan Wessel, Eliot Hazeltine, Atsushi Kikumoto, the members of the Cognitive Control Collaborative and the members of the Human Perception and Performance Group at the University of Iowa for helpful discussions.

Author Contributions

Conceptualization: J.J. and G.Y.; Data curation: G.Y.; Formal Analysis: J.J. and G.Y.; Funding acquisition: J.J.; Investigation: J.J. and G.Y.; Methodology: J.J. and G.Y.; Supervision: J.J.; Writing – original draft: G.Y.; Writing – review & editing: J.J. and G.Y.

Declaration of Interests

The authors declare no competing interests.

Materials and Methods

Subjects

We enrolled 36 participants. Two subjects were excluded due to lower than 70% accuracy in the test phase (see below). One more subject was excluded due to excessive head motion. The final sample consisted of 33 participants (18-42 years old, average of 25.0 ± 6.9 years; 22 females). All participants reported no history of psychiatric or neurological disorders, with normal or corrected-to-normal vision. The experiments were approved by the Institutional Review Board of the University of Iowa. Informed consent was obtained from all subjects prior to the experiment.

Experimental design

Training phase

The purpose of the training phase is to provide the participants with a set of rules (i.e., task sequences) to construct a rule-based strategy. Participants underwent training via an online web-based program to learn task transitions in sequences A (a→b→c→d→e) and B (d→c→a→e→b) (Fig. 4A). They performed multiple 5-trial mini-blocks to equip an avatar with gear based on a goal image (Fig. 1A). Each trial started with a sequence cue, succeeded by a goal image, a gear selection screen and feedback. To facilitate the learning of task transition, two test trials were administered after each mini-block, in which participants indicated the 1st/2nd/3rd task following a

cued task (Fig. S1). The training lasted 3-6 blocks and stopped when participants achieved a block-average accuracy of > 90% on test trials. Participants underwent the above training between 4-24 hours before scanning and performed another short repetition (1-2 blocks) immediately before scanning. For a detailed description, see Supplementary Note S4.

Test phase

In the test phase, the participants performed a new task that can be initially solved using the rules learned in the training phase. With practice, the task can also be solved using the memory-based strategy. The test phase was conducted in the scanner. The stimuli were back-projected onto a screen (with a viewing angle of ~14.0° between the equipment pictures and the center of the screen) behind the subject and viewed via a surface mirror mounted onto the head coil. On each trial, a cue with a letter and a number indicating the sequence and position (e.g. A4) was shown at the center of the screen (Fig. 1B). Six equipment images, representing the five equipment types and a foil (MOUSTACHE), were shown around the cue. The images were randomly selected from the two images of each equipment type. The locations of the six equipment types were randomized at the subject level but fixed within each subject. These fixed locations facilitate the implementation of the memory-based strategy. Participants were asked to select the equipment type representing the cued task with a pair of button pads, each assigned with three fingers (index, middle and ring fingers). The screen proceeded to a fixation for 8s if participants responded correctly, or to feedback for 1s and then a fixation for 7s if an error was made or no response was received within 9s following the cue. The test phase consisted of 6 blocks of 40 trials each.

Behavioral analysis

The analysis was centered on test phase data with RT and ER as dependent variables. For RTs, we excluded the error trials (4.4%), and trials with outlier RTs (> 3 SDs above the median, 1.5%). We constructed an LME model, with the block (1–6), position (1–4, which enabled the isolation of the clean effect of sequential recall by excluding position 5—known to involve a recency effect[37]), their interaction and intercept as fixed effects. Each slope and the intercept also included a random effect at the subject level. We used the “AOCTOOL” and “multcompare” functions in Matlab to compare the slopes of position between different blocks. For all LME models conducted in this study, we estimated the degree of freedom with the Satterthwaite approach.[38] For validation purposes, we expanded the analysis to include positions 1–5 (see Supplementary Note S1).

Computational Model

We built a computational model to simulate how the brain chooses between rule- and memory-based strategies using cost-benefit analysis. For the cost, the rule-based strategy has a cost C compared to the memory strategy:

$$C = L_t - i, \tag{1}$$

where L_t is the cued position (e.g., 4 in cue A4), and i is the sequence recall starting position. For example, when i is 1 and L_t is 4, the cost is 3 as there are 3 task transitions from position 1 to 4.

We operationalize the benefit as the probability of generating the correct response. For the rule-based strategy, as the participants have learned the transitions between steps from the training phase, the benefit depends on the strength of cue-task association at the starting position of the recall. For the memory strategy, the benefit relies on the strength of cue-task association at the cued position. Thus, for each sequence we modeled the cue-task association using a probabilistic distribution for each position i on each trial t as $M_{i,t}(j)$, which represents the model's belief that the task j is at position i. At the beginning of the experiment (i.e., $t = 0$), $M_{i,t}(j)$ was initialized in the following manner: For position 1, we assumed a perfect memory from the training phase with a probability of 1 for the correct task. For positions 2–4, a uniform distribution was used to simulate the situation of no informative cue-task associations. In position 5, the probability of the correct task received a boost of γ to account for the recency effect; all other tasks had the same probability. After each trial, the probability distribution $M_{i,t}$ is updated as a result of learning the correct task at the cued position using a delta rule:

$$M_{i,t}(j) = \begin{cases} M_{i,t}(j)+\alpha*(1-M_{i,t}(j)), \text{ if } j \text{ is the true task at position } i \\ M_{i,t}(j) - \frac{\alpha*(1-M_{i,t}(j))}{4}, \text{ if } j \text{ is another task} \end{cases}, \tag{2}$$

where α is the learning rate ranging from 0 to 1.

The memory strength index S is quantified as the reversed entropy of $M_{i,t}$:

$$S = -H(M_{i,t}) = \sum_{j=1}^{5} p_j * \log(p_j), \tag{3}$$

Note that a higher S indicates a stronger memory strength. Therefore, the quantified value (i.e., cost-benefit tradeoff) for starting recall at position i is:

$$V_{i,t} = \lambda * S - C = -\lambda * H(M_{i,t}) - (L_t - i), \tag{4}$$

where λ is the tradeoff between cost and benefit, ranging from 0.01 to 100. On trial t the decision of choosing the best recall starting position i^* is determined by:

$$i^* = \underset{i}{\operatorname{argmax}}\,(V_{i,t}), \tag{5}$$

When i^* is the cued position, memory strategy is implemented as no sequence recall is needed. When i^* is before the cued position, a rule-based strategy is selected.

Model fitting

We hypothesized that the RT for the rule and memory trials would be influenced by the rule implementation cost and memory strength, respectively. Therefore, we fit the

model outputs to the RT using a linear regression, which serves as the connection of the model predictions and behavior:

$$RT \sim C{*}Type_R + S{*}Type_M + Type_R + Type_M + C{*}Times_R + \log(Trial) + Response, \quad (6)$$

where the $Type_R$ and $Type_M$ encode the factors of rule and memory trials, respectively, while the $C{*}Times_R$ encodes the interaction between rule implementation cost and the aggregated number of recalled steps since the beginning of the experiment. The Response is a categorical factor encoding the response buttons. The objective function was defined as the residual sum of squares (RSS) from Eq. 6. To estimate the free parameters α, λ and γ, we ran the optimization 100 times (using fmincon in Matlab) with random starting values and chose the values led to the minimum RSS. To determine the best structure of the regression model, we compared this model to its reduced versions (Table 1) using the likelihood ratio test. The likelihood of each alternative model was estimated using an LME model incorporating data and predictors from all subjects. P values comparing the unrestricted model (M0) to each of the restricted models (M1–M5) were obtained through the ratio of likelihood, assessed against a chi-square null distribution, with degrees of freedom equal to the difference in the number of parameters between the two models. Comparisons between the alternative models were achieved using either the likelihood ratio test when they are nested or the Akaike information criterion (AIC) otherwise. The p value for the AIC comparison was estimated with exp(–ΔAIC/2) between two models.

To further test whether strategy selection is probabilistic or deterministic, we refined our model (M8) by incorporating a trial-wise weighting based on the certainty of the chosen strategy. Specifically, the weight W was calculated using a softmax function:

$$W = \frac{e^{V}}{e^{V_R} + e^{V_M}},$$

where V_R and V_M represent the values of rule- and memory-based strategies, respectively, while V denotes the expected value (either V_R or V_M, determined by the trial type) of each trial. As M8 predicts which strategy to use in a probabilistic manner, we used the probabilities as observation-level weights to predict RT using the same regression formula in Eq. 6. The regression analysis predicting behavioral RTs was conducted with the "lscov" function in Matlab. Other settings are the same as M0.

The "memory-threshold" hypothesis was tested with a new model (M9). Unlike previous models that decide between rule- and memory-based strategies, M9 specifically predicts that a transition to memory-based strategy occurs when its value exceeds a certain threshold (i.e., without comparing to the rule-based strategy). Therefore, we introduced a subject-specific free parameter θ (indicating the threshold), against which we compare the value of the memory-based strategy on each trial. This comparison determines whether to retain the rule-based strategy or switch to the memory-based strategy. In addition, we removed the parameter λ from M9, as it

does not involve direct comparisons between the two strategies. All other settings remain consistent with those of M0.

Behavioral transition point analysis

To estimate the group-level effect of post-strategy switch slowing,[19] we conducted an LME model using the trial type to predict RTs for the last rule and first memory trial. An intercept was added to capture the average RT. All predictors are treated as both the fixed effect and random effect at the subject level. Therefore, the model takes the following form:

$$RT = \beta_0 + \beta_1 TrialType + C + S + C*Times_R + \log(Trial) + RandomSlopes + \varepsilon, \quad (7)$$

where TrialType encodes either rule or memory trials, and RandomSlopes represents the random effect for the intercept and the slope of each fixed effect. We also estimated the null distribution for the post-strategy switch slowing by repeating the LME analysis using random permutation tests, in which transition points were shuffled 5,000 times. To test if the model inherently introduces the post-strategy switch slowing, we ran an additional permutation test by randomizing the model parameters 5,000 times. The p value was determined by the percentage of permutations inconsistent with the null hypothesis (e.g., with stronger or the same post-switch slowing than the real data in this test).

fMRI Image acquisition and preprocessing

Functional imaging was performed on a 7T GE 950 scanner using echo-planar imaging (EPI) sensitive to BOLD contrast [in-plane resolution of 1.7 × 1.7 mm^2, 128 × 128 matrix, 75 slices with a thickness of 2.0 mm and no interslice skip, repetition time (TR) of 1000 ms, multiband acceleration factor of 4, echo-time (TE) of 20.5 ms, and a flip angle of 50°]. In addition, a sagittal T1-weighted anatomical image was acquired as a structural reference scan, with a total of 512 slices at a thickness of 0.43 mm with no gap and an in-plane resolution of 0.70 × 0.43 mm^2.

Before preprocessing, the first eight volumes of the functional images were removed due to the unstable signals. The anatomical and functional data were preprocessed with the fMRIprep 22.0.2[39] (RRID:SCR_016216), which is based on Nipype 1.8.5[40] (RRID:SCR_002502). The BOLD time-series were resampled to the MNI152NLin2009cAsym space without smoothing. For a more detailed description of preprocessing, see Supplementary Note S5. After preprocessing, we resampled the functional data to a spatial resolution of 2 × 2 × 2 mm^3. The preprocessed data was smoothed with a full width at half maximum (FWHM) Gaussian kernel of 6 mm and 2mm for univariate and RSA, respectively. All analyses were conducted in volumetric space, and surface maps are produced with Connectome Workbench (https://www.humanconnectome.org/software/connectome-workbench) for display purposes only.

Estimation of fMRI activation

A generalized linear model (GLM) was conducted across six sessions (one for each block), with each session comprising trial-wise regressors time-locked to the onset of the cue. These regressors were convolved with a canonical hemodynamic response function (HRF) in SPM 12 (http://www.fil.ion.ucl.ac.uk/spm). We further added volume-level nuisance regressors, including the six head motion parameters, global signal, white matter signal, cerebrospinal fluid signal, and outlier TRs (defined as standard DVARS > 5 or frame-displacement > 0.9 mm from previous TR). Low-frequency signal drifts were filtered using a cutoff period of 128 s. The GLM yielded one beta map per trial, which was then noise normalized by dividing the original beta coefficients by the square root of the covariance matrix of the error terms.[41] The noise normalization was done separately for each of the 426 ROIs based on the extended Human Connectome Project multimodal parcellation atlas (HCPex, version 1.1[42]), resulting in one fMRI activation map for each trial. Error trials, outlier RT trials, and trials including large head movement volumes were excluded from further analysis. ROIs containing less than 50 voxels (i.e., 37 subcortical regions) were excluded from further analyses.

Multivariate regression analyses

We adopted a multivariate regression analysis approach from previous research[20] to quantify the representational strength of the cued position (representing rule implementation cost), memory strength, and the decision variable. The decision variable was operationalized as the absolute value difference (log-transformed) in $V_{i,t}$ (Eq. 4) between the two best values. The analysis was performed separately for each variable. In each analysis, a variable served as the main predictor, with the other two variables and behavioral RT as nuisance regressors. The analysis was conducted for each of the 426 ROIs, which underwent a 3-fold cross-validation procedure, where the data from 6 runs and the trial-wise variable time course were divided into chronological folds (2 runs per fold). Note that for the cued position effect, we only included participants who had rule trials in all blocks. For the training folds, trial-wise fMRI activity levels from each ROI were fitted to the variable time course using ridge regression [43] to prevent overfitting. The resulting weights were applied to the fMRI data in the test fold, generating a predicted variable time course. A stronger linear correlation between predicted and actual variable time courses indicated a robust representation of the variable in neural data. Following this, Fisher's transformation was applied to the three correlation coefficients obtained from each fold, and their mean served as the quantification of representational strength for the ROI.

For group-level analyses, we conducted a one-sample *t*-test against 0 for each ROI. Statistical results were corrected for multiple comparisons across all ROIs using the false discovery rate (FDR) method at the level of $q < 0.05$, with each individual ROI at uncorrected $p < .001$, both one-tailed (right).

RSA

For each ROI, the representational similarity between trials from different runs was defined as their voxel-wise correlation coefficient. Trial pairs from the same run were excluded due to their inflated similarity scores.[44,45] Vectorized representational similarity data were used as the dependent variable in the LME model analysis. In addition to fixed effects of interest, we added the intercept and two nuisance fixed effects encoding ROI-mean activation of each of the two trials to rule out the influence of activation strength on similarity score. Random effects consisted of the intercept and the slope for each fixed effect at the subject level. Statistical results were corrected for multiple comparisons across all the ROIs with FDR at the level of $q < 0.05$, with each individual ROI at uncorrected $p < 0.001$, both one-tailed. For detailed LME models, see Supplementary Note S7 and Fig. S5.

References

1. Fitts, P.M., and Posner, M.I. (1967). Human performance.
2. Anderson, J.R. (1982). Acquisition of cognitive skill. Psychological review *89*, 369-406. 10.1037/0033-295x.89.4.369.
3. Miller, E.K., and Cohen, J.D. (2001). An integrative theory of prefrontal cortex function. Annu Rev Neurosci *24*, 167-202. 10.1146/annurev.neuro.24.1.167.
4. Schneider, W., and Detweiler, M. (1988). A connectionist/control architecture for working memory. In Psychology of learning and motivation, (Elsevier), pp. 53-119.
5. Schuck, N.W., Gaschler, R., Wenke, D., Heinzle, J., Frensch, P.A., Haynes, J.D., and Reverberi, C. (2015). Medial prefrontal cortex predicts internally driven strategy shifts. Neuron *86*, 331-340. 10.1016/j.neuron.2015.03.015.
6. Dolan, Ray J., and Dayan, P. (2013). Goals and Habits in the Brain. Neuron *80*, 312-325. 10.1016/j.neuron.2013.09.007.
7. Evans, J.S., and Stanovich, K.E. (2013). Dual-Process Theories of Higher Cognition: Advancing the Debate. Perspect Psychol Sci *8*, 223-241. 10.1177/1745691612460685.
8. Evans, J.S.B.T. (2008). Dual-Processing Accounts of Reasoning, Judgment, and Social Cognition. Annual review of psychology *59*, 255-278. 10.1146/annurev.psych.59.103006.093629.
9. Kahneman, D. (2011). Thinking, fast and slow (macmillan).
10. Sheridan, H., and Reingold, E.M. (2017). Chess players' eye movements reveal rapid recognition of complex visual patterns: Evidence from a chess-related visual search task. J Vis *17*, 4. 10.1167/17.3.4.
11. van Opheusden, B., Kuperwajs, I., Galbiati, G., Bnaya, Z., Li, Y., and Ma, W.J. (2023). Expertise increases planning depth in human gameplay. Nature *618*, 1000-1005. 10.1038/s41586-023-06124-2.
12. Bilalic, M., Langner, R., Erb, M., and Grodd, W. (2010). Mechanisms and neural basis of object and pattern recognition: a study with chess experts. Journal of experimental psychology. General *139*, 728-742. 10.1037/a0020756.
13. Logan, G.D. (1988). Toward an instance theory of automatization. Psychological review *95*, 492-527. 10.1037/0033-295x.95.4.492.
14. Rickard, T.C. (1997). Bending the power law: A CMPL theory of strategy shifts and the automatization of cognitive skills. Journal of Experimental Psychology: General *126*, 288-311. 10.1037/0096-3445.126.3.288.
15. Shenhav, A., Botvinick, M.M., and Cohen, J.D. (2013). The expected value of control: an integrative theory of anterior cingulate cortex function. Neuron *79*, 217-240. 10.1016/j.neuron.2013.07.007.
16. Musslick, S., and Cohen, J.D. (2021). Rationalizing constraints on the capacity for cognitive control. Trends Cogn Sci *25*, 757-775. 10.1016/j.tics.2021.06.001.
17. Heathcote, A., and Matzke, D. (2022). Winner Takes All! What Are Race Models, and Why and How Should Psychologists Use Them? Current Directions in Psychological Science *31*, 383-394. 10.1177/09637214221095852.

18. Siegler, R.S. (1988). Strategy choice procedures and the development of multiplication skill. Journal of experimental psychology. General *117*, 258-275. 10.1037//0096-3445.117.3.258.
19. Lemaire, P., and Lecacheur, M. (2010). Strategy switch costs in arithmetic problem solving. Mem Cognit *38*, 322-332. 10.3758/MC.38.3.322.
20. Jiang, J., Wagner, A.D., and Egner, T. (2018). Integrated externally and internally generated task predictions jointly guide cognitive control in prefrontal cortex. Elife *7*. 10.7554/eLife.39497.
21. Kuhl, B.A., and Chun, M.M. (2014). Successful remembering elicits event-specific activity patterns in lateral parietal cortex. J Neurosci *34*, 8051-8060. 10.1523/JNEUROSCI.4328-13.2014.
22. Radvansky, G.A., and Zacks, J.M. (2017). Event Boundaries in Memory and Cognition. Curr Opin Behav Sci *17*, 133-140. 10.1016/j.cobeha.2017.08.006.
23. Yassa, M.A., and Stark, C.E.L. (2011). Pattern separation in the hippocampus. Trends Neurosci *34*, 515-525. 10.1016/j.tins.2011.06.006.
24. Mill, R.D., and Cole, M.W. (2023). Neural representation dynamics reveal computational principles of cognitive task learning. bioRxiv. 10.1101/2023.06.27.546751.
25. Lieder, F., and Griffiths, T.L. (2017). Strategy selection as rational metareasoning. Psychological review *124*, 762-794. 10.1037/rev0000075.
26. Shenhav, A., Musslick, S., Lieder, F., Kool, W., Griffiths, T.L., Cohen, J.D., and Botvinick, M.M. (2017). Toward a Rational and Mechanistic Account of Mental Effort. Annu Rev Neurosci *40*, 99-124. 10.1146/annurev-neuro-072116-031526.
27. Liu, Y., Dolan, R.J., Kurth-Nelson, Z., and Behrens, T.E.J. (2019). Human Replay Spontaneously Reorganizes Experience. Cell *178*, 640-652 e614. 10.1016/j.cell.2019.06.012.
28. Schuck, N.W., and Niv, Y. (2019). Sequential replay of nonspatial task states in the human hippocampus. Science *364*. 10.1126/science.aaw5181.
29. Wanjia, G., Favila, S.E., Kim, G., Molitor, R.J., and Kuhl, B.A. (2021). Abrupt hippocampal remapping signals resolution of memory interference. Nat Commun *12*, 4816. 10.1038/s41467-021-25126-0.
30. Jiang, J., Wang, S.F., Guo, W., Fernandez, C., and Wagner, A.D. (2020). Prefrontal reinstatement of contextual task demand is predicted by separable hippocampal patterns. Nat Commun *11*, 2053. 10.1038/s41467-020-15928-z.
31. Yang, G., Wu, H., Li, Q., Liu, X., Fu, Z., and Jiang, J. (2024). Dorsolateral prefrontal activity supports a cognitive space organization of cognitive control. Elife *12*. 10.7554/eLife.87126.
32. Nash, M.I., Hodges, C.B., Muncy, N.M., and Kirwan, C.B. (2021). Pattern separation beyond the hippocampus: A high-resolution whole-brain investigation of mnemonic discrimination in healthy adults. Hippocampus *31*, 408-421. 10.1002/hipo.23299.
33. Euston, D.R., Gruber, A.J., and McNaughton, B.L. (2012). The role of medial prefrontal cortex in memory and decision making. Neuron *76*, 1057-1070. 10.1016/j.neuron.2012.12.002.

34. Guise, K.G., and Shapiro, M.L. (2017). Medial Prefrontal Cortex Reduces Memory Interference by Modifying Hippocampal Encoding. Neuron *94*, 183-192 e188. 10.1016/j.neuron.2017.03.011.
35. Brown, T.I., Carr, V.A., LaRocque, K.F., Favila, S.E., Gordon, A.M., Bowles, B., Bailenson, J.N., and Wagner, A.D. (2016). Prospective representation of navigational goals in the human hippocampus. Science *352*, 1323-1326. 10.1126/science.aaf0784.
36. Bowman, C.R., and Zeithamova, D. (2018). Abstract Memory Representations in the Ventromedial Prefrontal Cortex and Hippocampus Support Concept Generalization. J Neurosci *38*, 2605-2614. 10.1523/jneurosci.2811-17.2018.
37. Talmi, D., and Goshen-Gottstein, Y.J.M. (2006). The long-term recency effect in recognition memory. *14*, 424-436.
38. Satterthwaite, F.E. (1946). An Approximate Distribution of Estimates of Variance Components. Biometrics Bulletin *2*. 10.2307/3002019.
39. Esteban, O., Markiewicz, C.J., Blair, R.W., Moodie, C.A., Isik, A.I., Erramuzpe, A., Kent, J.D., Goncalves, M., DuPre, E., Snyder, M., et al. (2019). fMRIPrep: a robust preprocessing pipeline for functional MRI. Nat Methods *16*, 111-+. 10.1038/s41592-018-0235-4.
40. Gorgolewski, K., Burns, C.D., Madison, C., Clark, D., Halchenko, Y.O., Waskom, M.L., and Ghosh, S.S. (2011). Nipype: a flexible, lightweight and extensible neuroimaging data processing framework in python. Frontiers in neuroinformatics *5*, 13. 10.3389/fninf.2011.00013.
41. Walther, A., Nili, H., Ejaz, N., Alink, A., Kriegeskorte, N., and Diedrichsen, J. (2016). Reliability of dissimilarity measures for multi-voxel pattern analysis. NeuroImage *137*, 188-200. 10.1016/j.neuroimage.2015.12.012.
42. Huang, C.C., Rolls, E.T., Feng, J., and Lin, C.P. (2022). An extended Human Connectome Project multimodal parcellation atlas of the human cortex and subcortical areas. Brain Struct Funct *227*, 763-778. 10.1007/s00429-021-02421-6.
43. Xue, G., Dong, Q., Chen, C., Lu, Z., Mumford, J.A., and Poldrack, R.A. (2010). Greater neural pattern similarity across repetitions is associated with better memory. Science *330*, 97-101. 10.1126/science.1193125.
44. Cai, M.B., Schuck, N.W., Pillow, J.W., and Niv, Y. (2019). Representational structure or task structure? Bias in neural representational similarity analysis and a Bayesian method for reducing bias. PLoS Comput Biol *15*, e1006299. 10.1371/journal.pcbi.1006299.
45. Mumford, J.A., Davis, T., and Poldrack, R.A. (2014). The impact of study design on pattern estimation for single-trial multivariate pattern analysis. Neuroimage *103*, 130-138. 10.1016/j.neuroimage.2014.09.026.